The maximum likelihood climate change for global warming under the influence of greenhouse effect and Lévy noise

Cite as: Chaos **30**, 013132 (2020); https://doi.org/10.1063/1.5129003
Submitted: 27 September 2019 . Accepted: 17 December 2019 . Published Online: 21 January 2020

Yayun Zheng, Fang Yang, Jinqiao Duan, Xu Sun, Ling Fu, and Jürgen Kurths

The maximum likelihood climate change for global warming under the influence of greenhouse effect and Lévy noise

Cite as: Chaos **30**, 013132 (2020); doi: 10.1063/1.5129003
Submitted: 27 September 2019 · Accepted: 17 December 2019 ·
Published Online: 21 January 2020

View Online Export Citation CrossMark

Yayun Zheng,[1,2,3] Fang Yang,[1] Jinqiao Duan,[4,a)] Xu Sun,[1] Ling Fu,[2] and Jürgen Kurths[2,3,5]

AFFILIATIONS

[1]School of Mathematics and Statistics and Center for Mathematical Science, Huazhong University of Science and Technology, Wuhan 430074, China
[2]Wuhan National Laboratory for Optoelectronics, Huazhong University of Science and Technology, Wuhan 430074, China
[3]Potsdam Institute for Climate Impact Research, Potsdam 14473, Germany
[4]Department of Applied Mathematics, Illinois Institute of Technology, Chicago, Illinois 60616, USA
[5]Department of Physics, Humboldt University, Berlin 12489, Germany

[a)]**Author to whom correspondence should be addressed:** duan@iit.edu

ABSTRACT

An abrupt climatic transition could be triggered by a single extreme event, and an α-stable non-Gaussian Lévy noise is regarded as a type of noise to generate such extreme events. In contrast with the classic Gaussian noise, a comprehensive approach of the most probable transition path for systems under α-stable Lévy noise is still lacking. We develop here a probabilistic framework, based on the nonlocal Fokker-Planck equation, to investigate the maximum likelihood climate change for an energy balance system under the influence of greenhouse effect and Lévy fluctuations. We find that a period of the cold climate state can be interrupted by a sharp shift to the warmer one due to larger noise jumps with low frequency. Additionally, the climate change for warming 1.5 °C under an enhanced greenhouse effect generates a steplike growth process. These results provide important insights into the underlying mechanisms of abrupt climate transitions triggered by a Lévy process.

Abrupt climatic transitions happened several times in the past, but their mechanisms are poorly understood. Here, we argue that such a transition from one climate state to another could be triggered by a single extreme event, and an α-stable non-Gaussian Lévy noise is regarded as the general type of noise to generate such extreme events. We develop a probabilistic framework to quantify the maximum likelihood transition path. The probability density for transition sample paths is expressed by solutions of the associated nonlocal Fokker-Planck equation, thus avoiding the difficulty for obtaining the action functional as in the Onsager-Machlup methodology or the assumption of a sufficiently small noise intensity like in large deviation theory. Our approach is applied to a paradigmatic energy balance system under the combined influence of the greenhouse effect and Lévy fluctuations. We examine the maximum likelihood climate change for a global warming of 1.5 °C, which is as required by the Paris Agreement. We verify that the maximum likelihood abrupt transition path in the climatic change energy balance system could be triggered by α-stable Lévy noise. Furthermore, we uncover that the global surface temperature increases stepwise with a transfer rate under an enhanced greenhouse effect. We expect the maximum likelihood path as an efficient research tool, which quantitatively describes how the climate changes, and explain how the greenhouse effect combined with Lévy noise affect the warming of the Earth.

I. INTRODUCTION

A rare but most influential phenomenon in climate change is a sharp shift from one climate state to another.[1] In particular, the last glacial period experienced rapid, decadal-scale transitions 20 times from a stadial cold state to an interstadial warm one, called Dansgaard-Oeschger events.[2–4] The oxygen isotope ($\delta^{18}O$) profiles

from Greenland ice cores are shown in Fig. 8 of Appendix A. There have been a number of views on the mechanisms behind such abrupt changes. One proposed explanation for such events is that they happened when the Earth system reached a critical tipping point.[5–7] Tipping points are associated with bifurcations or induced by noise. Meanwhile, the interaction of ocean thermohaline circulation, ice shelf, and sea ice feedbacks are used to explain DO cycles.[8,9]

There is an alternative view that the abrupt climatic changes could be triggered by extreme events, such as heat waves, droughts, floods, hurricanes, blizzards, and other events that occur rarely.[1,10–12] Ditlevsen argued that the paleoclimatic records indicate that random fluctuations in a rapid transition have a strong non-Gaussian distribution with a heavy tail and intermittent jumps,[10,13] and an α-stable Lévy process is thought to be an appropriate model for such a non-Gaussian process.[14] We will, therefore, consider α-stable non-Gaussian Lévy noise in the following study. Although early-warning signals are detected for an upcoming catastrophic change,[15–17] it is extremely difficult to predict a sudden transition. The identification and characterization of the states along the path of the dynamics is the crucial step to explore such abrupt shift events, where a curve connecting two states in the state space is a transition pathway. Our goal then is to study the maximal likely transition path for a climate change model under α-stable Lévy fluctuations.

There are several available methods to investigate transitions in stochastic systems with Gaussian noise. For small-noise-induced transitions, the Freidlin-Wentzell theory of large deviations is often utilized. The minimizer of the Freidlin-Wentzell action functional provides the most probable pathway and the occurrence rate of the rare events.[18,19] For stochastic systems with a finite noise intensity, the path integral provides the expression of the conditional propagator for studying the most probable transition path.[20] This most probable transition path can also be approximated by minimizing the Onsager-Machlup action functional.[21,22] For the diffusion process, the maximum *a posteriori* estimator is given by the solution of an appropriate variational problem.[23] Particularly, in a gradient system, the most probable path follows the minimum energy, which passes through the unstable manifold at some saddle points.[24]

Note that numerous studies mentioned above focused on diffusion processes. These processes are the solutions of stochastic differential equations (SDEs) with the (Gaussian) Brownian motion. However, the abrupt climate changes seem to occur intermittent with high probability, where the dynamics become strongly non-Gaussian in contrast to the case of Gaussian noise.[10] Unfortunately, it is difficult to obtain the corresponding action functional from existing research results when it comes to dealing with the transition paths in stochastic systems with non-Gaussian Lévy fluctuations. Although the Onsager-Machlup action functional for stochastic dynamical systems under Lévy noise is derived recently by one of us,[25] the results are valid only for certain Lévy fluctuations. Therefore, it is desirable to develop a framework for describing the transition paths of stochastic dynamical systems under non-Gaussian noise, especially α-stable Lévy noise.

Our approach uses the Fokker-Planck equations for non-Gaussian dynamical systems. These are deterministic equations describing how probability density functions propagate and evolve. The nonlocal or fractional Laplacian operator in these equations is the manifestation of α-stable Lévy fluctuations. Recently, we developed a fast and accurate numerical algorithm to simulate nonlocal Fokker-Planck equations under either absorbing or natural conditions.[26] Meanwhile, we derived the Fokker-Planck equations for Marcus SDEs driven by Lévy processes.[27] We also used a nonlocal Zakai equation to examine the most probable path for systems with α-stable Lévy systems and continuous-time observations.[28] Furthermore, we devised most probable phase portraits to capture certain aspects of stochastic dynamics[29] and applied to examine qualitative changes or bifurcation of equilibrium states under Lévy noise.[30]

In order to determine the maximum likelihood transition path between two states, we will derive the expression for the conditional probability density $p(x,t|x_0,0;x_f,t_f)$ and for sample paths with initial condition $X(0)=x_0$ and a final condition $X(t_f)=x_f$ (i.e., sample paths connecting the two states x_0 and x_f). The maximizer $x_m(t)$, at each time instant t, for the conditional probability density $p(x,t|x_0,0;x_f,t_f)$ indicates the maximal likely location of the sample paths (see Sec. II B). Taking all times on $[0,t_f]$, the set of maximizers $x_m(t)$ constitutes a transition path. It can be referred to as the maximum likelihood transition path between two states x_0 and x_f. It is only a set of x_m, which makes the density function $p(x,t|x_0,0;x_f,t_f)$ maximum. To illustrate this approach of the maximum likelihood transition path, we will study an energy balance climatic system driven by a discontinuous (with jumps) α-stable Lévy process (Sec. II D). Numerical experiments are conducted to investigate the impact of the non-Gaussianity and greenhouse factor on the maximum likelihood transition path between a cold glacial state and a warm interstadial state in Sec. III. Finally, the paper is summarized in Sec. IV and accompanied with Appendixes A–D.

II. METHODS AND MODEL

In this section, we introduce the Fokker-Planck equation for the transition probability density. For the sake of explanation, we consider the following SDE with a constant noise intensity $\eta>0$:

$$\mathrm{d}X(t)=f(X(t))\mathrm{d}t+\eta\mathrm{d}N(t),\quad X(0)=x_0\in\mathbb{R}^d, \tag{1}$$

where $X(t)=(X_1(t),X_2(t),\ldots,X_d(t))$ is a $\mathbb{R}^d$-valued stochastic process and $f:\mathbb{R}^d\to\mathbb{R}^d$ is Lipschitz continuous. The $\mathbb{R}^d$-valued noise process $N(t)$ is either a standard Brownian motion $B(t)$ or a symmetric α-stable Lévy process with the Lévy index $\alpha\in(0,2)$. The detailed introduction for the α-stable Lévy process is given by Appendix C.

A. Fokker-Planck equation for the transition probability density $Q(x,t\,|\xi,s)$

Two types of probability density expressions are introduced: $p(X(t)=u)$ is a general case to represent the density for the $\mathbb{R}^d$-valued solution $X(t)$ of SDE at $X(t)=u$, and $Q(u,t|\xi,s)$ is reserved to denote the transition density, which is defined as $Q(\cdot,\cdot|\cdot,\cdot):\mathbb{R}^d\times[0,t_f]|\mathbb{R}^d\times[0,t_f]\to[0,\infty)$. For example, $Q(u,t|\xi,s)$ with $0\leqslant s<t\leqslant t_f$ represents the density of $X(t)$ at $X(t)=u$ given $X(s)=\xi$. It can be expressed in terms of p,

$$Q(u,t|\xi,s)=p(X(t)=u|X(s)=\xi).$$

We suppose that for each $x_0\in\mathbb{R}^d$, SDE (1) has a unique strong solution, and the probability density for this solution exists and is strictly positive. Then, the transition probability density

$Q(x,t|\xi,s)$ for (1) with Brownian motion $[N(t)=B(t)]$ satisfies a Fokker-Planck equation,[31]

$$\frac{\partial}{\partial t}Q(x,t|\xi,s) = -\sum_{i=1}^{d}\frac{\partial}{\partial x_i}(f_i(x)Q(x,t|\xi,s)) + \frac{\eta^2}{2}\sum_{i,j=1}^{d}\frac{\partial^2}{\partial x_i x_j}Q(x,t|\xi,s). \quad (2)$$

The transition probability density for (1) driven by an α-stable Lévy motion $[N(t)=L_t^\alpha]$ satisfies the following nonlocal Fokker-Planck equation:[32]

$$\frac{\partial}{\partial t}Q(x,t|\xi,s) = -\sum_{i=1}^{d}\frac{\partial}{\partial x_i}(f_i(x)Q(x,t|\xi,s)) + \eta^\alpha\int_{\mathbb{R}^d\setminus\{0\}}Q(x+y,t|\xi,s)-Q(x,t|\xi,s)\nu_\alpha(dy) - \eta^\alpha\int_{\mathbb{R}^d\setminus\{0\}}\sum_{i=1}^{d}\frac{\partial}{\partial x_i}I_{\|y\|<1}yQ(x,t|\xi,s)]\nu_\alpha(dy). \quad (3)$$

The integral part of the right-hand side is actually the nonlocal or fractional Laplacian operator, reflecting the non-Gaussian α-stable Lévy fluctuations.[32] Both of them fulfill the same initial condition,

$$\lim_{t\to s}Q(u,t|\xi,s)=\delta(u-\xi).$$

B. The maximum likelihood transition path

We propose our approach to determine and investigate the maximum likelihood transition path from one state to another for dynamical systems under non-Gaussian α-stable Lévy noise. Inspired by Lemma 3.2 in the reference,[33] for all $t\in[0,t_f]$ and $x,x_0,x_f\in\mathbb{R}^d$, we assume that the conditional probability density $\mathscr{P}_A(x,t)$ is defined in a (x,t,p)-space and is used to describe the probability density of SDE (1); i.e., X_t is located at the position x at time t subjecting to condition A. Here, x is a state in the full phase space in which the dynamics is Markovian, the subscript A is used to indicate the special type of constraint with the initial condition $X(0)=x_0$, and the final condition $X(t_f)=x_f$. It can be expressed as

$$\mathscr{P}_A(x,t) = p(X(t)=x|X(0)=x_0;X(t_f)=x_f) = \frac{Q(x_f,t_f|x,t)Q(x,t|x_0,0)}{Q(x_f,t_f|x_0,0)}, \quad (4)$$

where transition probability density Q is the solution of the associated Fokker-Planck equation with the appropriate initial condition as mentioned in Sec. II A. The detailed derivation is given in Appendix A. Subjecting to condition A, the density function $\mathscr{P}_A(x,t)$ has a peak at a time $t\in[0,t_f]$, and the peak corresponds to a state $x_m(t)$. It implies that, at a given time instant t, the maximizer $x_m(t)$ for the conditional probability density $\mathscr{P}_A(x,t)$ indicates the maximum likelihood location of these stochastic trajectories (or sample paths). That is, we find the state $x_m(t)$ by maximizing the transition probability density $\mathscr{P}_A(x,t)$,

$$x_m(t)=\arg\max_x \mathscr{P}_A(x,t). \quad (5)$$

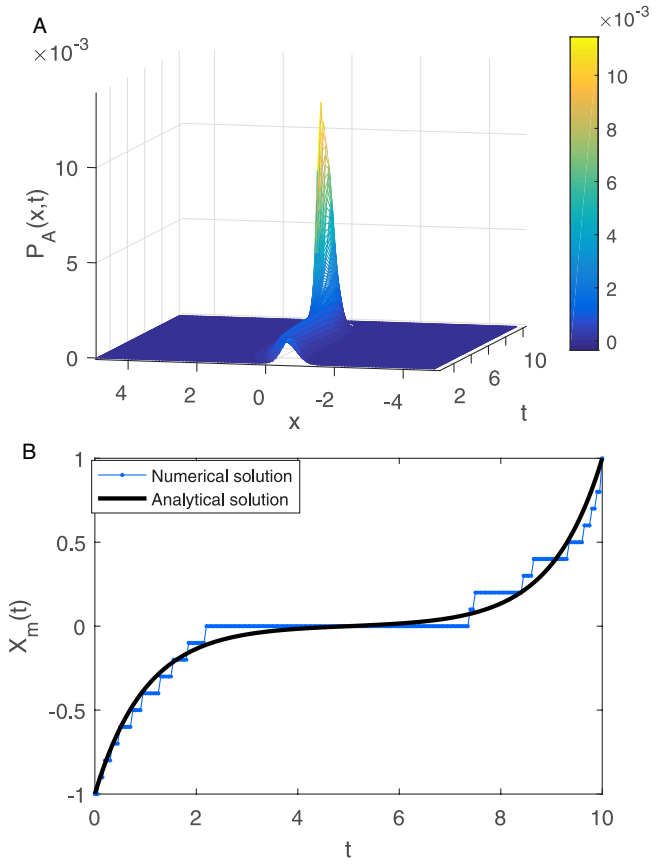

FIG. 1. The maximum likelihood transition path. (a) The conditional probability density function $\mathscr{P}_A(x,t)$ for a scalar Ornstein-Uhlenbeck process (see Appendix B). (b) The numerical simulation of the maximum likelihood transition path is compared with the analytical solution.

Now, we examine the corresponding transition behavior by the expression of the conditional probability density $\mathscr{P}_A(x,t)$ in Eq. (D1), in a simple example. In Fig. 1(a), the conditional probability density $\mathscr{P}_A(x,t)$ for a scalar Ornstein-Uhlenbeck process $X(t)$ [Eq. (B1)] can be simulated by the numerical algorithm of Gao *et al.*[26] (see Appendix D). Meanwhile, we examine that the numerical simulation for the maximum likelihood path $x_m(t)$ is valid by comparing the numerical solution Eq. (5) (the dashed line) with the analytical solution (the solid line), as shown in Fig. 1(b). The calculation of the analytical solution is described in Appendix B.

C. Energy balance model

We have thus developed a probabilistic framework for describing the maximum likelihood transition path between two states. This technique is now applied to study a climate energy balance model

[Eq. (6)] for examining the maximum likelihood climate change. Climate change is represented here by the global mean surface temperature $T(t)$ evolution throughout the entire system.[34,35] The heat capacity C defines as the amount of heat that must be added to the object to raise its temperature. The global energy change is expressed by the difference between the incoming solar radiative energy E_{in} and the outgoing radiative energy E_{out} at time t,

$$C\frac{\mathrm{dTdt}}{=}\frac{1}{4}(1-\alpha(T))S_0-\gamma\theta T^4. \tag{6}$$

The incoming energy $E_{in}=1/4(1-\alpha(T))S_0$ is the total amount of solar radiation absorbed by our planet after surface reflection with the solar constant $S_0=1368\,\mathrm{W\,m^{-2}}$. The planetary albedo $\alpha(T)$ independence on temperature is expressed as[35]

$$\alpha(T)=0.5-0.2\tanh\left(\frac{T-265}{10}\right).$$

For the energy E_{out}, the earth is simply assumed to behave approximately as a blackbody radiator with an effective surface temperature T, for which the energy is given by the Stefan-Boltzmann law θT^4 with the Stefan constant $\theta=5.67\times10^{-8}\,\mathrm{Wyr\,m^{-2}}$. Meanwhile, the greenhouse effect is a natural process that warms Earth's surface. The absorbed energy by greenhouse gases causes the global average temperature to rise.[36,37] To maintain an energy balance, the greenhouse factor $\gamma\in[0,1]$ is used to express the outgoing energy reduction $E_{out}=\gamma\theta T^4$. Equation (6) can be written as $\dot{T}=-U'(T)$ with the potential function,

$$U(T)=\left(-\frac{1}{4}S_0\left(0.5T+2\ln\left(\cosh\left(\frac{T-265}{10}\right)\right)\right)+\frac{1}{5}\gamma\theta T^5\right)/C.$$

It is difficult to obtain the analytical solutions of the equilibrium temperature T in Eq. (6), but the approximate solutions could be received as following if $\tanh x$ can be expanded as Taylor series $\tanh T=T-T^3/3+o(T)$:

$$T_{eq}=-\frac{0.0912}{4a}+\frac{\pm\sqrt{\kappa+2y}\pm\sqrt{-(3*\kappa+2y\pm\frac{2\xi}{\sqrt{\kappa+2y}})}}{2},$$

where $a=2.27\times10^{-7}\gamma$, $\kappa=-0.25/8a^2-72.5/a$, and $\xi=7.58\times10^{-4}/8a^3+6.12/2a^2+1.92\times10^4/a$. The y can be expressed by $y=-5/6\kappa-G/3M+M$ with $\tau=-2.07\times10^{-4}/256a^4-0.603/16a^3-1.75\times10^3/4a^2-1.69\times10^6/a$ $M=-\kappa/12-\tau$, $K=-\kappa^3/108+\kappa\tau/3-\xi^2/8$, and $G=\sqrt[3]{K/2\pm\sqrt{K^2/4+M^3/27}}$.

D. Stochastic energy balance model

Hasselmann's[38] idea is that the short-timescale fluctuating processes, such as wind above the ocean surface, modeled as stochastic processes, can be thought of as driving long-term climate variations. From analyzing paleoclimatic data, Ditlevsen[10,39] shows that such fast timescale noise contains a component with an α-stable distribution. Extreme events, such as heat waves, droughts, and storms as triggering mechanisms for climatic changes, can be represented by α-stable Lévy noise.[10] Therefore, a type of a more realistic energy balance model with underlying extreme events can be written as

$$\frac{\mathrm{dT}}{\mathrm{dt}}=\frac{1}{C}\left(\frac{1}{4}(1-\alpha(T))S_0-\gamma\theta T^4\right)+\frac{\tilde{\varepsilon}}{C}\dot{L}_t^{\alpha}. \tag{7}$$

Here, $\dot{L}_t^{\alpha}$ is a Lévy noise, which can be modeled by a scalar symmetric α-stable Lévy process with the generating triplet $(0,0,\nu_\alpha)$, i.e., a pure jump motion with $0<\alpha<2$ (see Appendix C). On the other hand, the "normal" atmospheric fluctuations effected on the energy balance system are modeled by Gaussian noise $\dot{B}_t$,

$$\frac{\mathrm{dT}}{\mathrm{dt}}=\frac{1}{C}\left(\frac{1}{4}(1-\alpha(T))S_0-\gamma\theta T^4\right)+\frac{\tilde{\sigma}}{C}\dot{B}_t, \tag{8}$$

where $\tilde{\varepsilon}/C=\varepsilon$ and $\tilde{\sigma}/C=\sigma$ are the noise intensities of the α-stable Lévy process and Brownian motion, respectively.

III. RESULTS

We start the detailed analysis for the energy balance model (6) by examining the equilibrium temperature states: $\mathrm{dT/dt}=0$. The equilibria against the greenhouse effect γ show on the S-shaped curve in Fig. 2(a). The two turning points γ_f^* and γ_h^* mark the critical parameter values for which branches of equilibria meet and vanish. During the bistable region ($\gamma_h^*<\gamma<\gamma_f^*$), the deterministic climatic system exhibits the two stable states at T_s and an unstable state at T_u by the potential functions $U(T)$, such as $\gamma=0.51$ and 0.67 shown in Fig. 2(b). Assuming that the greenhouse effect γ increases in the bistable region, the temperature of the colder glacial state and warmer interstadial state is decreasing, which causes Earth's temperature to drop. At $\gamma_f^*\approx0.688\,46$, there is only one stable state $T=226.5\,\mathrm{K}$ ($-40.65\,^\circ\mathrm{C}$); i.e., the climate will reflect the long-time stabilization in an ice-covered state called "Snowball Earth."[40] In contrast, as the greenhouse factor γ decreases, the temperature of the stable equilibrium states increases until the greenhouse effect becomes strong enough at $\gamma_h^*\approx0.49$, and the Earth will then remain in a high temperature environment $T=304.7\,\mathrm{K}$ ($31.5\,^\circ\mathrm{C}$). Thus, the greenhouse factor values γ_f^* and γ_h^* are referred to as *deep freeze bifurcation* and *desert heat bifurcation*, respectively.[41] These imply that the global surface temperature T increases as the greenhouse factor γ decreases. Therefore, the decreased greenhouse factor enhances the greenhouse effect and causes a rise in the global mean surface temperature.

The climate change of underlying extreme events can be modeled by the stochastic energy balance system (7) driven by a symmetric α-stable Lévy process. Here, the α-stable Lévy process L_t^{α} is a pure jump process defined by a stable Lévy process with $0<\alpha<2$. Next, we discuss the impact of α-stable Lévy noise on the climate change. The corresponding change behavior of the global temperature is present by numerical simulation of the maximum likelihood transition path $x_m(t)$ in Eq. (5).

A. Effect of α-stable Lévy noise for a global warming of 1.0 °C

The heat capacity $C=46.8\,\mathrm{Wyr\,m^{-2}}$ is regarded as a weighted average value of ocean and land surface warming by 1.0 °C.[37] We investigate the pathway of climate change starting in a cold glacial

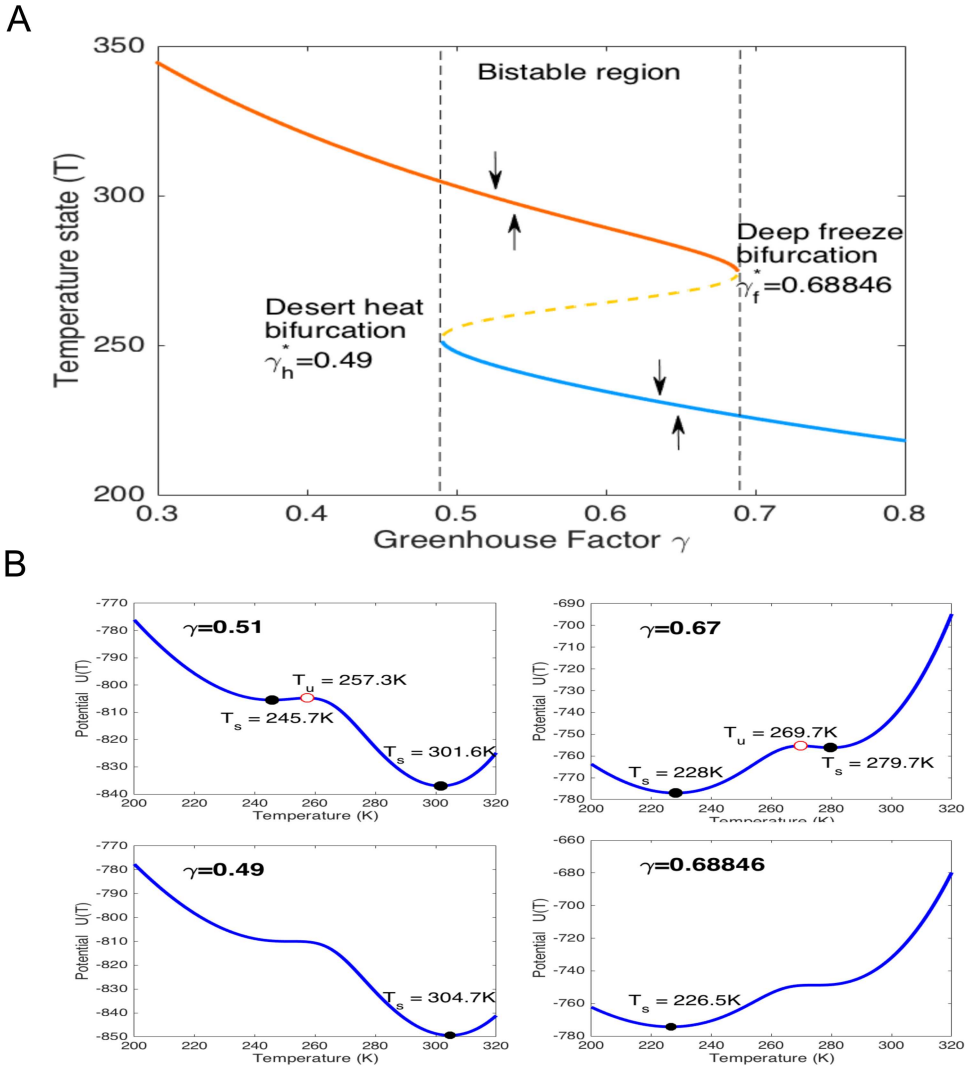

FIG. 2. The energy balance model [Eq. (6)] may have multiple equilibria. (a) The bifurcation diagram as the greenhouse factor γ varies. (b) The potential functions $U(T)$ for greenhouse factors: $\gamma = 0.51$, $\gamma_h^* = 0.49$, $\gamma = 0.67$, and $\gamma_f^* = 0.688\,46$.

state and landing in a warmer interstadial state when the climate system is triggered by a single extreme event. The simulation for the maximum likelihood transition path is described in Appendix D. Two kinds of typical greenhouse factors near the bifurcation points are chosen, such as $\gamma = 0.51$ and $\gamma = 0.67$, each of them has two stable states as shown in Fig. 2(b). The numerical results of the maximum likelihood transition path are presented with different amounts of α-stable Lévy noise intensities $\varepsilon = 0.1, 1, 3,$ and 5 in Fig. 3. It is well known that the α-stable Lévy process has larger jumps with lower jump probabilities for α close to 0, while it has smaller jumps with higher frequencies for a large value of α [$\alpha \in (1, 2)$]. Here, we compared the transition path for two representative values of the Lévy index $\alpha = 0.5$ and $\alpha = 1.5$.

First, we consider the maximum likelihood transition path from the cold glacial state ($T = 245.7$ K) to the warmer interstadial one ($T = 301.6$ K) for $\gamma = 0.51$ as shown in Fig. 3(a). We choose the bounded domain $D = (208\,\text{K}, 308\,\text{K})$ because the size of the basin of the cold glacial state is equal to the warmer one. For small values of ε ($\varepsilon \leqslant 1$), we find that a period of a relatively stable cold glacial state is interrupted by a sharp transition to the warmer interstadial state. The path of the maximum likelihood transition is not obviously different between $\alpha = 0.5$ and $\alpha = 1.5$. A significant difference is presented as ε is increasing, such as $\varepsilon = 3$ and 5. For $\alpha = 0.5$, we find that there is a sudden jump when the global surface temperature gradually increases from the cold state to the warmer one. However, for $\alpha = 1.5$, the path of climate change presents an almost continuous growth curve as $\varepsilon = 5$. The results on the maximum likelihood transition path show that one has to consider both the values of ε and α when deciding which of the three competing factors plays a vital role in the climate change system, the noise intensity, the jump frequency, or the jump size.

Next, Fig. 3(b) illustrates the behavior of the maximum likelihood transition for $\gamma = 0.67$ from the ice-cover state ($T = 228$ K) to the warmer interstadial one ($T = 279.7$ K). Given a bounded

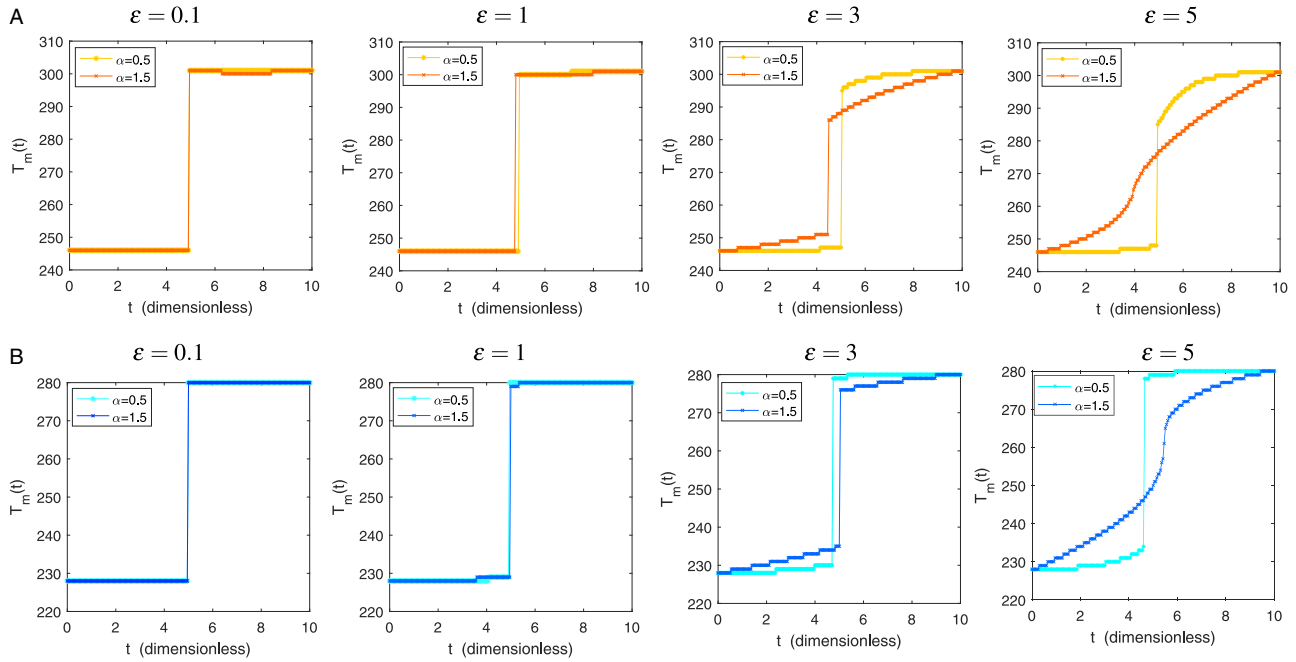

FIG. 3. The dependence of the maximum likelihood transition path on the α-stable Lévy noise intensities ε for global warming 1.0 °C. The maximum likelihood path for (a) $\gamma = 0.51$ (transition from the cold climate stable state $T = 245.7$ K to the warmer one $T = 301.6$ K) and (b) for $\gamma = 0.67$ (transition from the deep-frozen climate stable state $T = 228$ K to the warmer one $T = 279.7$ K) with $\alpha = 0.5$ and $\alpha = 1.5$.

domain $D = (220\,\text{K}, 320\,\text{K})$ with the same size of the attraction basin of the cold and warmer state, we uncover that the climate likely experiences a rapid increase followed by a long-time stable trend for small noise intensities. This change behavior is in agreement with the corresponding result for $\gamma = 0.51$. However, for $\gamma = 0.67$, an obvious difference is the transferring time to the warmer state.

Furthermore, we examine the effect of the Lévy noise intensity ε and the Lévy motion index α on transition time from the colder state to the warmer one for $\gamma = 0.51$ and 0.67. Figure 4(a) shows that for smaller jumps with higher jump probabilities, such as $\alpha = 1.5$, the transition time t_m increases as ε is raised for the case of $\gamma = 0.67$, while $\gamma = 0.51$ has the opposite behavior. The reason is that the potential of the cold state is larger than the warmer one for $\gamma = 0.51$; thus, the climate change system is easier to shift from higher to lower. Note that for $\alpha = 0.5$, the critical shift points are reached nearing $t = t_f/2$ for both $\gamma = 0.51$ and $\gamma = 0.67$. On the other hand, we consider the transition time t_m when α is increasing while keeping $\varepsilon = 0.5$ and 3. For a small noise intensity $\varepsilon = 0.5$, the transition times are concentrated around $t_f/2$ as α increases. For a larger noise intensity $\varepsilon = 3$, the behavior of transition time does not change monotonically; instead, the t_m first increases, reaches a maximum at $\alpha = 0.5$, and then decreases with increasing α for $\gamma = 0.51$. Meanwhile, $\gamma = 0.67$ also has a similar behavior; the difference is that it exists a minimum t_m at the same value of α. These results imply that we could find the optimal transition times for these two parameters ε and α when the greenhouse factor is fixed.

B. Effect of α-stable Lévy noise for a global warming of 1.5 °C

Due to human activities, the world has already warmed by 1.0 °C since the preindustrial times. The Intergovernmental Panel on Climate Change's (IPCC) special report on the impact of a global warming of 1.5 °C has caught broad attention. According to the report, the global warming is likely to reach 1.5 °C between the year 2030 and 2052 if we continue to increase greenhouse gas emission at the current rate.[42]

Meanwhile, we look at the effect of warming 1.5 °C on the climate change with the heat capacity $C = 70.27\,\text{Wyrm}^{-2}$. We reveal that the maximum likelihood transition paths for a global warming of 1.5 °C have a similar behavior to the case of 1.0 °C as mentioned in Sec. III A (Fig. 3). Clearly, the climate dynamics subjecting to a small value of α, such as $\alpha = 0.5$, experience occasional sharp transition from one state to another. Meanwhile, the transition path presents a nearly continuous trend attributing to small jumps combined with a larger noise intensity, such as $\alpha = 1.5$ and $\varepsilon = 5$. On the other hand, there are some subtle differences when the global warms 1.5 °C, such as $\gamma = 0.51$ with $\varepsilon = 3$ and $\alpha = 0.5$. In contrast to the temperature continuing to increase in the case of warming 1.0 °C [Fig. 3(a)], the temperature for warming 1.5 °C has a performance of a rapid decrease followed by a slow increase after a sudden shift as shown in Fig. 5(a). Meanwhile, for a weakened greenhouse effect, such as $\gamma = 0.67$, we observe that the global surface temperature continues to rise for $\varepsilon = 5$ and $\alpha = 1.5$ as shown in Fig. 5(b), rather than a

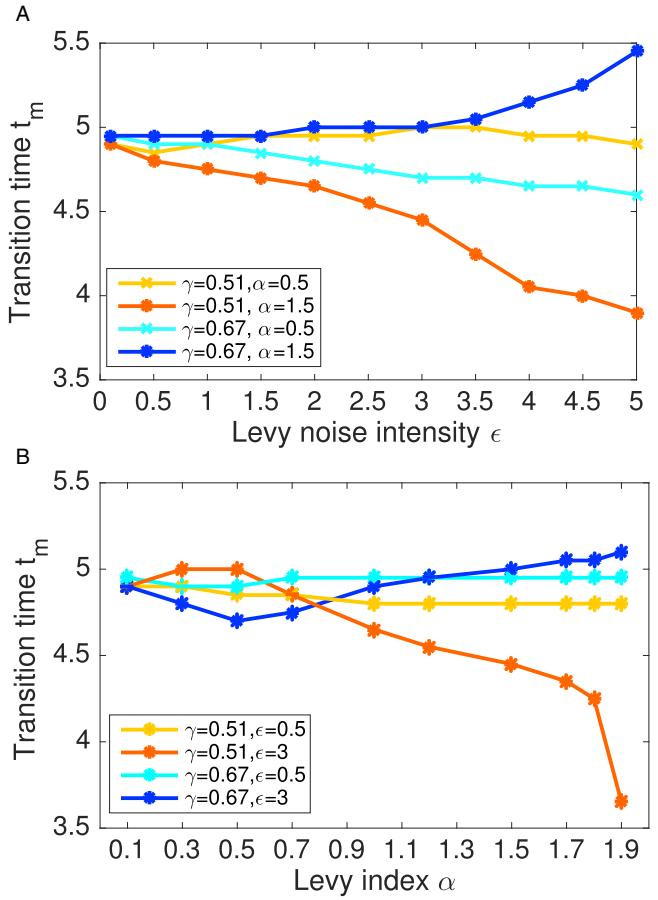

FIG. 4. Transition time T_m for bistable greenhouse factors $\gamma = 0.51$ and $\gamma = 0.67$. (a) Effect of the Levy noise intensity ε on transition times with $\alpha = 0.5$ and 1.5. (b) Effect of the Levy motion index α on transition times with $\varepsilon = 0.5$ and 3.

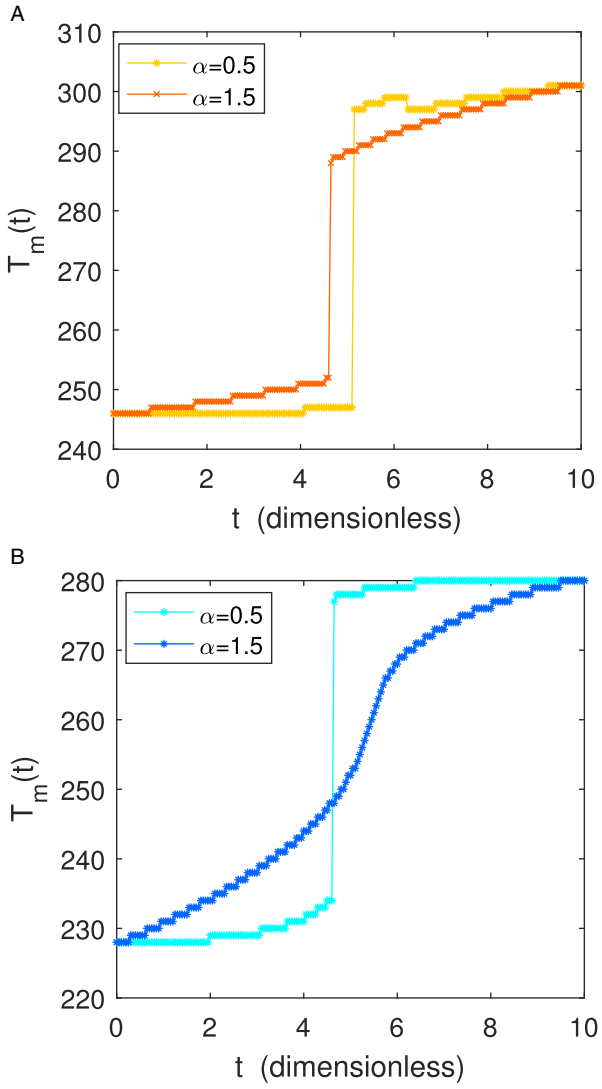

FIG. 5. The dependence of the maximum likelihood transition path on the α-stable Lévy noise intensities ε for global warming 1.5 °C. (a) $\gamma = 0.51$ (transition from the cold stable state $T = 245.7$ K to the warmer one $T = 301.6$ K) with $\varepsilon = 3$ and (b) $\gamma = 0.67$ (transition from the deep-frozen state $T = 228$ K to the warmer one $T = 279.7$ K) with $\varepsilon = 5$.

sudden shift in the case of warming 1.0 °C [Fig. 3(b)]. These results imply that it is more likely to induce multiple abrupt climate changes with global warming under an enhanced greenhouse effect, while the sudden transfer phenomenon will be replaced by continuous changes for the weakened greenhouse effect when the global surface temperature warms to 1.5 °C. This also reflects the importance of reducing greenhouse gas emissions.

Comparing the maximum likelihood transition paths for $\gamma = 0.51$ and $\gamma = 0.67$, we find that the growth of the temperature for $\gamma = 0.67$ tends to be slow, before or after an abrupt transition with varying parameters ε and α. It means that the weakened greenhouse effect ($\gamma = 0.67$) may be slowing down the climate change. This is the reason why we need to reduce and even cut complete emissions of the greenhouse gas. The tendency of slow warming may help people to gain time to adapt to extreme climate, such as heat waves, droughts, and flooding.

Furthermore, we focus on how the climate changes from the current temperature state to the high-temperature one for a global warming of 1.5 °C. To illustrate such question, we examine the effect of α-stable Lévy noise on the maximum likelihood transition path from a current state $T = 290$ K (the global average temperature in April 2019) to a warmer state. The warmer state is considered as the stable state $T = 304.7$ K of the desert heat bifurcation $\gamma_h^* = 0.49$, which corresponds to the enhanced greenhouse effect.

In Fig. 6, we find that the maximum likelihood transition path is a steplike process increasing to the warmer state from the current one. For $\alpha = 0.5$, the global surface temperature manifests itself as a stepwise slowly increases followed by an abrupt shift,

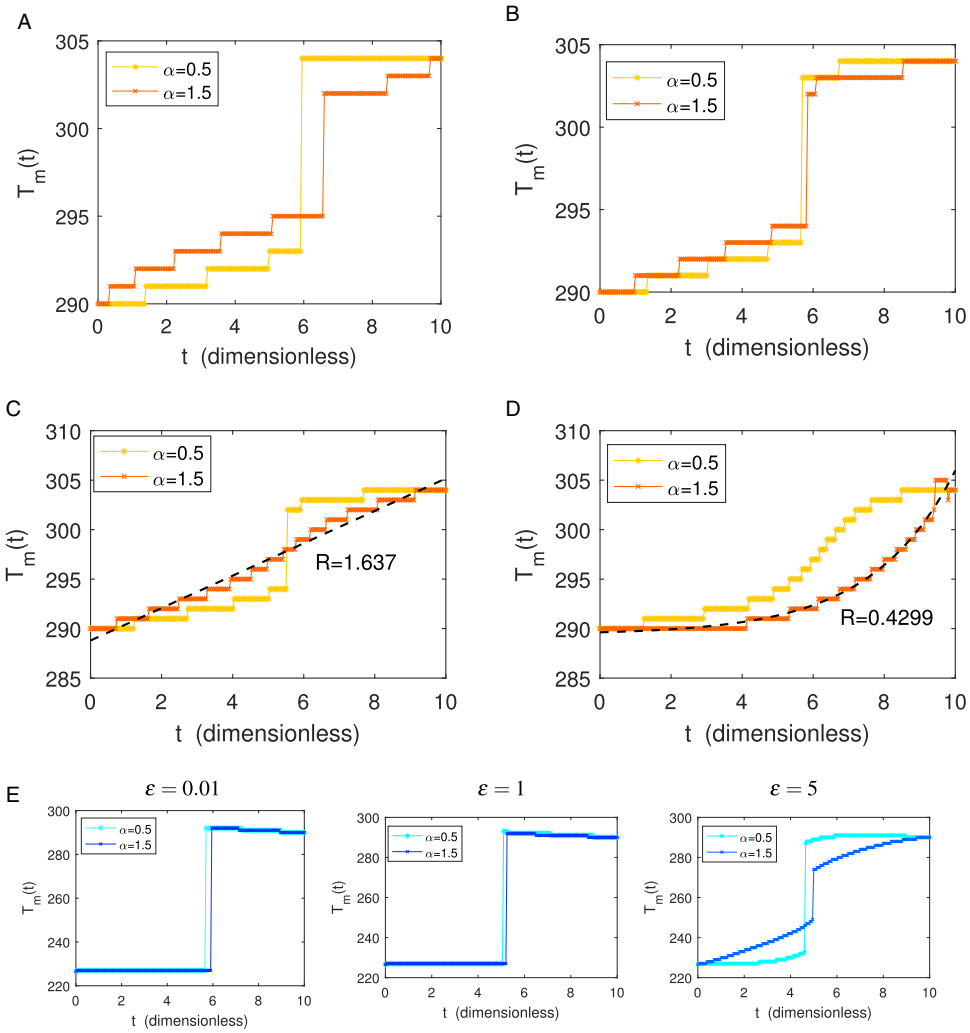

FIG. 6. The effect of α-stable Lévy noise intensities on the maximum likelihood transition path for the bifurcation greenhouse factor. Transition from the current state 290 K to the stable state 304.7 K of desert heat bifurcation $\gamma_h^* = 0.49$ with (a) $\varepsilon = 0.01$. (b) $\varepsilon = 0.1$. (c) $\varepsilon = 1$. (d) $\varepsilon = 5$. (e) Transition from the stable state 226.5 K of deep-frozen bifurcation $\gamma_f^* = 0.688\,46$ to the current state 290 K.

and the magnitude of the sudden jump gradually decreases as the ε increases. In contrast, for a larger α, such as $\alpha = 1.5$, the temperature is increasing linearly for $\varepsilon = 1$ with the transfer rate $R = 1.637$ as shown in Fig. 6(c). We give an expression of the linear growth by curve fitting with 0.95 confidence bounds,

$$T_m(t) = 1.637t + 288.8.$$

Figure 6(d) shows that the climate change is not a simple linear relationship with time t when the noise intensity ε increases to 5. The temperature maintains around the current state at the outset and then the growth rate changes slowly and then stabilizes at the warmer state $T = 304.7$ K. In view of such characteristics, an exponential growth function is proposed to fit the climate change,

$$T_m(t) = 0.2252e^{0.4299t} + 289.4.$$

In the following discussion, we pay attention to the maximum likelihood pathways of climate change from a frozen state to the current state; due to a global warming of 1.5 °C, the collapse of ice sheets leads to a rise in the sea level. In Fig. 6(e), we look at the effect of α-stable Lévy noise on the maximum likelihood path transition from the stable state $T = 226.5$ K of the deep-frozen bifurcation $\gamma_f^* = 0.688\,46$ to the current one $T = 290$ K. In comparison with the "linear" growth of temperature for the greenhouse factor $\gamma = 0.51$, we find that the maximum likelihood path for the greenhouse factor $\gamma = 0.67$ always presents a sudden transition between two states even for a larger noise intensity ε. The global surface temperature maintains in the frozen state for a period of time, and then it declines slowly to the current temperature after a sudden jump.

C. Effect of the Gaussian noise

Having discussed the maximum likelihood transition path under α-stable Lévy noise, we now examine the effect of Gaussian noise on the maximum likelihood pathway. Figure 7 shows that the maximum likelihood path has a similar transition behavior

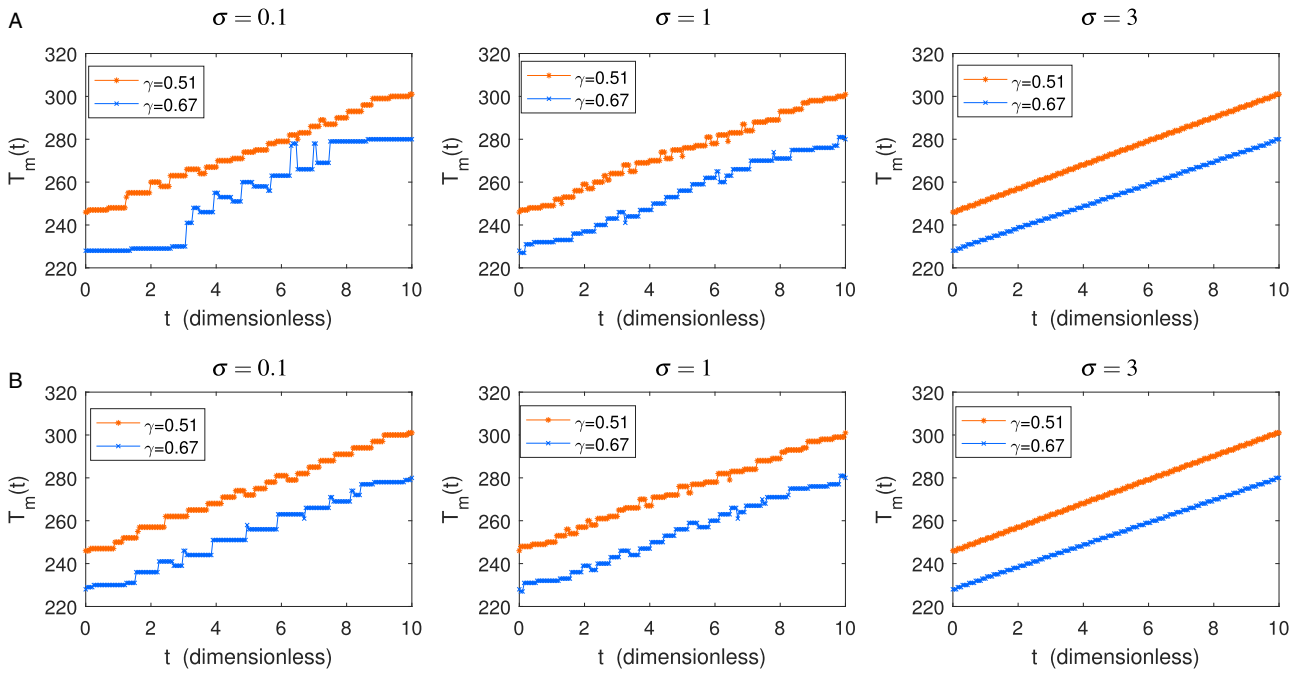

FIG. 7. The effect of Gaussian noise on the maximum likelihood transition path. The greenhouse factors $\gamma = 0.51$ and $\gamma = 0.67$ for (a) a global warming of 1.0 °C and for (b) a global warming of 1.5 °C, with varying noise intensities $\sigma = 0.1, 1,$ and 3.

for a global warming of 1.0 °C and 1.5 °C, respectively, with the varying Gaussian noise intensity σ. In contrast to sharp transition under non-Gaussian α-stable Lévy noise, we find that the global surface temperatures under Gaussian noise are gradually increasing along with small fluctuations. Moreover, the temperature increases steadily in a linear fashion in the case of the noise intensity $\sigma = 3$. For a small value of σ, such as $\sigma = 0.1$, the fluctuation amplitude at the greenhouse factor $\gamma = 0.67$ is larger than that at the greenhouse factor $\gamma = 0.51$.

IV. CONCLUSION

To understand the mechanism of an abrupt transition in climate change, we have proposed an approach, based on transition probability densities and nonlocal Fokker-Planck equations, to investigate the maximum likelihood transition path from a stadial cold state to an interstadial warm one under α-stable Lévy noise. The maximum likelihood transition path $x_m(t)$ is defined as the maximizer of the conditional probability density function $\mathscr{P}_A(x,t)$, for each time instant t, subject to an initial condition $X(0) = x_0$ and a final condition $X(t_f) = x_f$.

Our approach has the following advantages over the existing methods for examining the most probable transition paths: (i) Our approach expresses the probability density for transition sample paths via solutions of the associated Fokker-Planck equation and thus avoids the difficulty for obtaining the action functional in the Onsager-Machlup approach, in systems with pure α-stable Lévy noise.[21,25] (ii) Our approach applies to systems with either Gaussian or non-Gaussian noise and is not an asymptotic method, and thus, we avoid the assumption of a sufficiently small noise intensity (which is required in the large deviation approach[18]). (iii) Our approach applies while a path integral representation for systems with non-Gaussian Lévy noise is not yet generally available, as noted in our earlier work.[43]

Applying our approach to a climate energy balance system under the interaction of the greenhouse effect and α-stable Lévy noise, we examine the maximum likelihood climate change for global warming of 1.0 °C and 1.5 °C, respectively. Numerical simulations have revealed the delicate dependence of the climate change on the noise intensity, jump frequency, and jump size for various greenhouse factors. We find that a period of the relatively stable climate has been interrupted by sharp transitions to the warmer state attributing to larger jumps with lower frequency. Such a phenomenon implies that **the discontinuous jumps of the α-stable Lévy process may be thought as the underlying mechanism leading to an abrupt shift.** Meanwhile, comparing with two typical greenhouse factors nearing bifurcation points, we discover that the weakened greenhouse effect ($\gamma = 0.67$) is more effective in slowing down the climate change.

The greenhouse gas emissions related to the global warming of 1.5 °C have significant influences on humanity and ecosystems. Furthermore, we uncover that the maximum likelihood path for an enhanced greenhouse effect generates a steplike growth

process, as transferring from the current temperature state to the high-temperature one. Moreover, we find that the global surface temperature stepwise increases with an exponential transfer rate for a larger noise intensity combined with small jumps. However, for the weakened greenhouse effect, the climate suddenly reaches the warmer interstadial state in which it has been for a long time at the frozen state.

Finally, as a comparison, we have also examined the maximum likelihood climate change when the energy balance system is under Gaussian fluctuations. The global surface temperature is gradually increasing by changing in small fluctuations. The continuous sample paths could explain why the climate models with Gaussian fluctuations cannot succeed in describing sudden shifts between climatic states.

ACKNOWLEDGMENTS

We would like to thank Xiaoli Chen, Xiujun Cheng, and Yang Liu for discussions about computation. This work was supported by the NSFC grants (Nos. 11801192 and 1620449), Leibniz-DAAD research fellowships [No. 2018(57423756)], and the Hubei provincial postdoctoral science and technology activity project.

APPENDIX A: THE DERIVATION OF THE CONDITIONAL PROBABILITY DENSITY IN Eq. (D1)

We assume that SDE (1) has a unique strong solution, the probability density for this solution exists and is strictly positive, and then the conditional density of $X(t)$ given for both values of $X(0)$ and $X(t_f)$ exists. In fact, by the Markov property of SDE (1), the density is exactly the same as the density of $X(t_f)$ under the condition that only the value of $X(t)$ is given, i.e.,

$$p(X(t_f) = x_f|X(0) = x_0; X(t) = x) = p(X(t_f) = x_f|X(t) = x) = Q(x_f, t_f|x, t). \tag{A1}$$

The conditional density of $X(t)$ is given by

$$\begin{aligned} p(X(t) = x|X(0) = x_0; X(t_f) = x_f) &= \frac{p(X(t) = x; X(0) = x_0; X(t_f) = x_f)}{p(X(0) = x_0; X(t_f) = x_f)} \\ &= \frac{p(X(t_f) = x_f|X(0) = x_0; X(t) = x)p(X(t) = x|X(0) = x_0)}{p(X(t_f) = x_f|X(0) = x_0)}. \end{aligned} \tag{A2}$$

Equation (A2) indicates that the density for $X(t)$ defined by SDE (1) exists with respect to the condition $X(0) = x_0$ and $X(t_f) = x_f$, and the right-hand side of Eq. (A2) is well defined by the assumption. Substituting Eq. (A1) into Eq. (A2) and changing the notation p to Q, we obtain the expression for the probability density function $\mathscr{P}_A(x, t)$,

$$\begin{aligned} \mathscr{P}_A(x, t) &= p(X(t) = x|X(0) = x_0; X(t_f) = x_f) \\ &= \frac{Q(x_f, t_f|x, t)Q(x, t|x_0, 0)}{Q(x_f, t_f|x_0, 0)}. \end{aligned} \tag{A3}$$

Thus, a governing equation for the transition probability density $\mathscr{P}_A(x, t)$ of the solution of SDEs (1) is derived; see Fig. 1(a).

APPENDIX B: A SIMPLE EXAMPLE WITH AN ANALYTICAL SOLUTION FOR THE MAXIMUM LIKELIHOOD TRANSITION PATH

In order to verify that the numerical scheme is valid, the numerical solution is compared with the analytical solution for the maximum likelihood transition path $x_m(t)$. We consider the following Ornstein-Uhlenbeck SDE with additive Gaussian noise:

$$\mathrm{d}X(t) = -aX(t)\mathrm{d}t + b\mathrm{d}B_t, \quad X(0) = x_0 \in \mathbb{R}^1, \tag{B1}$$

where a and b are real parameters. In the special case of (B1), we let $a = 1$, $b = 0.1$, $x_0 = -1$, $x_f = 1$, $t_f = 10$, and a bounded domain $D = (-5, 5)$. Based on the expression of the conditional probability density $\mathscr{P}_A(x, t)$ in Eq. (D1), we may calculate the density function

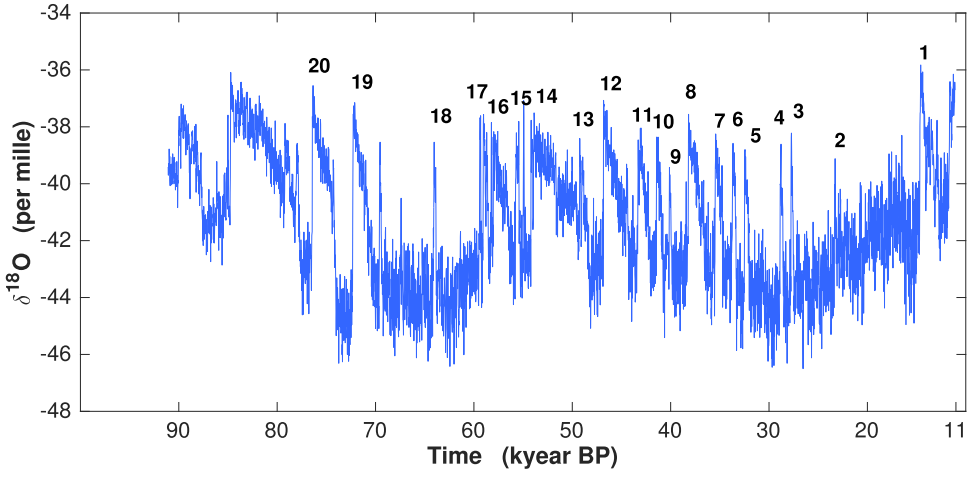

FIG. 8. The Dansgaard-Oeschger (DO) events. The NGRIP ice core δ^{18}O record[2] from Greenland during the time interval between 11 000 and 90 000 years before present.

$Q(x,t|x_0,0)$ of SDE (B1),

$$Q(x,t|x_0,0)=\frac{\sqrt{a}}{\sqrt{\pi b^2(1-e^{-2at})}}\exp\left[-\frac{a(x-e^{-at}x_0)^2}{b^2(1-e^{-2at})}\right],$$

and the other density function $Q(x_f,t_f|x,t)$ is given by

$$Q(x_f,t_f|x,t)=\frac{\sqrt{a}}{\sqrt{\pi b^2(1-e^{-2a(t_f-t)})}}\exp\left[-\frac{a(x_f-e^{-a(t_f-t)}x)^2}{b^2(1-e^{-2a(t_f-t)})}\right],$$

since the production of the density function $Q(x_f,t_f|x,t)Q(x,t|x_0,0)$ is a strictly increasing function with x; thus, the maximum exists in a bounded domain. The derivatives of the density function with respect to x, i.e., the analytical solution, are solved,

$$x_{\max}(t)=\frac{(e^{-a(t_f-t)}-e^{-a(t_f+t)})x_f+(e^{-at}-e^{-a(2t_f-t)})x_0}{1-e^{-2at_f}}.$$

The numerical solution $x_{\max}(t)$ can be simulated via the numerical global optimization of $\mathscr{P}_A(x,t)$ [Eq. (D1)] by the numerical algorithm of Gao *et al.*[26]; see Fig. 1(b).

APPENDIX C: THE α-STABLE LÉVY PROCESS

The well-known Brownian motion is a Gaussian process, with stationary and independent increments and almost surely continuous sample paths. A Lévy process L_t is a non-Gaussian process, with stationary and independent increments; i.e., for any s,t with $0\le s\le t$, the distribution of $L(t)-L(s)$ only depends on $t-s$, and for any partition $0=t_0<t_1<\cdots<t_n=t$, $L(t_i)-L(t_{i-1})$, $i=1,2,\ldots,n$ is independent. The sample paths of the Levy process are almost surely right continuous with left limits (*càdlàg*),[32] and as a result, the sample paths have countable jumps. Lévy processes are thought as appropriate models for non-Gaussian fluctuations with heavy-tailed statistical distributions and intermittent bursts. The characteristic function for a Lévy process in $\mathbb{R}^d$ with a generating triplet (b,Q,ν) is given by the Lévy-Khintchine formula,[44]

$$Ee^{i<\lambda,L_t>}=\exp\left\{it<b,\lambda>-t\frac{1}{2}<\lambda,Q\lambda>+t\int_{\mathbb{R}^d\setminus\{0\}}(e^{i<\lambda,y>}-1-i<\lambda,y>I_{\|y\|<1}y)\nu(dy)\right\},\tag{C1}$$

where the notation $<\cdot,\cdot>$ is the inner product in $\mathbb{R}^d$ and the I_S is the indicator function of the set S. Thus, the Lévy process is characterized by a vector $b\in\mathbb{R}^d$, a positive definite symmetric $d\times d$ matrix Q, and a Lévy jump measure ν defined on $\mathbb{R}^d\setminus\{0\}$ satisfying

$$\int_{\mathbb{R}^d\setminus\{0\}}(\|y\|^2\wedge 1)\nu(dy)<\infty.$$

The Lévy jump measure quantifies the jump frequency and size for sample paths of this Lévy process.

An α-stable Lévy process L_t^α is a special type of the Lévy process defined by the stable Lévy random variable with the distribution $S_\alpha(\delta,\beta,\lambda)$. Usually, $\alpha\in(0,2)$ is called the Lévy index (non-Gaussianity index), $\delta\in[0,\infty)$ is the scale parameter, $\beta\in[-1,1]$ is the skewness parameter, and $\lambda\in(-\infty,\infty)$ is the shift parameter.

A stable Lévy random variable L^α has the following "heavy tail" estimate:

$$\lim_{y\to\infty}y^\alpha\mathbb{P}(L^\alpha>y)=C_\alpha\frac{1+\beta}{2}\sigma^\alpha;$$

i.e., the tail estimate decays in a power law. The constant C_α depends on α.

In particular, for a symmetric α-stable Lévy process L_t^α with the generating triplet $(0,0,\nu_\alpha)$, the characteristic function becomes

$$Ee^{i<\lambda,L_t^\alpha>}=e^{-t\|\lambda\|^\alpha},\quad t>0,\lambda\in\mathbb{R}^d,$$

with the jump measure[14]

$$\nu_\alpha(dy)=\frac{C(\alpha,d)}{\|y\|^{n+\alpha}}dy.$$

The constant $C_{\alpha,d}$ depends on α and dimension d. The α-stable Lévy motion L_t^α has larger jumps with lower jump probabilities for α is small ($0<\alpha<1$), while it has smaller jumps with higher jump frequencies for large α values ($1<\alpha<2$). The special case $\alpha=2$ corresponds to the usual Brownian motion, which is a Gaussian process. For more information on α-stable Lévy motions, see Refs. 14, 32, and 44.

APPENDIX D: SIMULATION FOR THE MAXIMUM LIKELIHOOD TRANSITION PATH

The conditional probability density $\mathscr{P}_A(x,t)$ is related to the transition density $Q(x_f,t_f|x,t)$ of reaching the target state x_f and the transition density $Q(x,t|x_0,0)$ of starting at the initial state x_0. Therefore, the numerical calculation for $\mathscr{P}_A(x,t)$ can be converted into the calculation of the product of $Q(x_f,t_f|x,t)$ and $Q(x,t|x_0,0)$. Each of them satisfies the Fokker-Planck equations (2) or (3). The main simulation problem is how to find a solution in a nonlocal Fokker-Planck equation (3). In the present paper, we apply the "punched-hole" trapezoidal numerical algorithm of Gao *et al.*[26] to solve the fractional operator under the absorbing condition.

This numerical algorithm is generalized for our model [Eq. (7)] in $x\in D$ on $\mathbb{R}^1$. The choice of domain D depends on the different stable states for the greenhouse factor. The transitional density $Q(x,t|x_0,0)$ represents the density of $X(t)$ at $X(t)=x$ given $X(0)=x_0$. We can simply decompose the integral of the probability density Q [Eq. (3)] into three parts $\int_{\mathbb{R}^1}=\int_{-\infty}^{a-x}+\int_{b-x}^{a-x}+\int_{b-x}^{+\infty}$ in $\mathbb{R}^1$ and analytically evaluate the first and third integrals,

$$Q_t=-(f(x)Q)_x-\frac{\varepsilon^\alpha C_\alpha}{\alpha}\left[\frac{1}{(x-a)^\alpha}+\frac{1}{(b-x)^\alpha}\right]Q+\varepsilon^\alpha C_\alpha\int_{a-x}^{b-x}\frac{Q(x+y,t)-Q(x,t)}{|y|^{1+\alpha}}dy,\tag{D1}$$

for $x\in(a,b)$. The α-stable symmetric jump measure is

$$\nu_\alpha(dy)=C_\alpha|y|^{-(1+\alpha)}dy,$$

where the constant C_α is defined as $C_\alpha=\frac{\alpha}{2^{1-\alpha}\sqrt{\pi}}\Gamma(\frac{1+\alpha}{2})\Gamma(1-\frac{\alpha}{2})$. The Lévy motion index is $\alpha\in(0,2)$, and the Lévy intensity constant is ε. The integral $\int_{\mathbb{R}^1}\frac{I_{|y|<1}(y)yp'}{|y|^{1+\alpha}}dy$ has been dropped because this term

does not have any effect on the numerical results.[45] In the numerical simulations, the probability profile of its initial position is the Gaussian $p(x,0) = \sqrt{\frac{40}{\pi}} e^{-40x^2}$. We have chosen the spatial resolution $h = 0.02$ and the time step size $\triangle t = 0.5h^2$. The absorbing condition implies that the density will vanish once it is out of a bounded domain $D = (a, b)$,

$$p(x,t) = 0 \quad \text{for} \quad x \notin (a,b).$$

Finally, the maximum likelihood states $X_m(t)$ can be found via numerical optimization of $\mathscr{P}_A(x,t)$. For numerical optimization, we use Matlab's built-in function *find*, which returns the indices of the product of $Q(x_f, t_f|x,t)$ and $Q(x,t|x_0,0)$, that is, the maximum for $x \in (a,b)$.

It is worth pointing out how to determine the arrival time t_f. For different random sample trajectories starting at x_0, the time when the system reached the state x_f is different. The optimization problem related to the most probable transition path and time t_f is employed by the theory of large deviations.[46] Here, the arrival time t_f can be determined by Monte Carlo simulations, which calculate the average time of arriving at state x_f or by the first mean exit time starting at state x_0 from an interval D as in our earlier work.[47] We emphasize here that the time $t \in [0, 10]$ is dimensionless.

REFERENCES

[1] National Research Council, *Abrupt Impacts of Climate Change: Anticipating Surprises* (National Academies Press, 2013).
[2] I. K. Seierstad, P. M. Abbott, M. Bigler, T. Blunier, A. J. Bourne, E. Brook, S. L. Buchardt, C. Buizert, H. Clausen, E. Cook *et al.*, "Consistently dated records from the Greenland GRIP, GISP2 and NGRIP ice cores for the past 104 ka reveal regional millennial-scale $\delta^{18}O$ gradients with possible Heinrich event imprint," Quat. Sci. Rev. **106**, 29–46 (2014).
[3] W. Dansgaard, S. Johnsen, H. Clausen, D. Dahl-Jensen, N. Gundestrup, C. Hammer, C. Hvidberg, J. Steffensen, A. Sveinbjörnsdottir, J. Jouzel *et al.*, "Evidence for general instability of past climate from a 250-kyr ice-core record," Nature **364**, 218 (1993).
[4] W. Dansgaard, S. J. Johnsen, H. B. Clausen, D. Dahl-Jensen, N. Gundestrup, C. U. Hammer, and H. Oeschger, "North Atlantic climatic oscillations revealed by deep Greenland ice cores," Clim. Process. Clim. Sensit. **29**, 288–298 (1984).
[5] P. Ashwin, S. Wieczorek, R. Vitolo, and P. Cox, "Tipping points in open systems: Bifurcation, noise-induced and rate-dependent examples in the climate system," Philos. Trans. R. Soc. A **370**, 1166–1184 (2012).
[6] T. M. Lenton, H. Held, E. Kriegler, J. W. Hall, W. Lucht, S. Rahmstorf, and H. J. Schellnhuber, "Tipping elements in the Earth's climate system," Proc. Natl. Acad. Sci. U.S.A. **105**, 1786–1793 (2008).
[7] S. Bathiany, H. Dijkstra, M. Crucifix, V. Dakos, V. Brovkin, M. S. Williamson, T. M. Lenton, and M. Scheffer, "Beyond bifurcation: Using complex models to understand and predict abrupt climate change," Dyn. Stat. Clim. Syst. **1**(1), dzw004 (2016).
[8] N. Boers, M. Ghil, and D. D. Rousseau, "Ocean circulation, ice shelf, and sea ice interactions explain Dansgaard–Oeschger cycles," Proc. Natl. Acad. Sci. U.S.A. **115**, E11005–E11014 (2018).
[9] A. Clement and L. Peterson, "Mechanisms of abrupt climate change of the last glacial period," Rev. Geophys. **46**, RG4002, https://doi.org/10.1029/2006RG000204 (2008).
[10] P. D. Ditlevsen, "Observation of α-stable noise induced millennial climate changes from an ice-core record," Geophys. Res. Lett. **26**, 1441–1444, https://doi.org/10.1029/1999GL900252 (1999).
[11] J. Knox and Z. Kundzewicz, "Extreme hydrological events, palaeo-information and climate change," Hydrological Sci. J. **42**, 765–779 (1997).
[12] Á. Corral and Á. González, "Power law size distributions in geoscience revisited," Earth Space Sci. **6**(5), 673–697 (2019).
[13] P. Ditlevsen, "Climate transitions on long timescales," Contemp. Phys. **50**, 511–532 (2009).
[14] K. I. Sato, *Lévy Processes and Infinitely Divisible Distributions* (Cambridge University Press, 1999).
[15] V. Dakos, M. Scheffer, E. van Nes, V. Brovkin, V. Petoukhov, and H. Held, "Slowing down as an early warning signal for abrupt climate change," Proc. Natl. Acad. Sci. U.S.A. **105**, 14308–14312 (2008).
[16] M. Scheffer, J. Bascompte, W. A. Brock, V. Brovkin, S. R. Carpenter, V. Dakos, H. Held, E. H. Van Nes, M. Rietkerk, and G. Sugihara, "Early-warning signals for critical transitions," Nature **461**, 53 (2009).
[17] T. M. Lenton, "Early warning of climate tipping points," Nat. Clim. Chang. **1**, 201 (2011).
[18] M. I. Freidlin and A. D. Wentzell, "Random perturbations," in *Random Perturbations of Dynamical Systems* (Springer, 1998).
[19] X. Wan and G. Lin, "Hybrid parallel computing of minimum action method," Parallel Comput. **39**, 638–651 (2013).
[20] K. L. C. Hunt and J. Ross, "Path integral solutions of stochastic equations for nonlinear irreversible processes: The uniqueness of the thermodynamic Lagrangian," J. Chem. Phys. **75**, 976–984 (1981).
[21] D. Dürr and A. Bach, "The Onsager-Machlup function as Lagrangian for the most probable path of a diffusion process," Commun. Math. Phys. **60**, 153–170 (1978).
[22] L. Onsager and S. Machlup, "Fluctuations and irreversible processes," Phys. Rev. **91**, 1505 (1953).
[23] O. Zeitouni and A. Dembo, "A maximum a posteriori estimator for trajectories of diffusion processes," Stochastics **20**, 221–246 (1987).
[24] D. V. Berkov, "Numerical calculation of the energy barrier distribution in disordered many-particle systems: The path integral method," J. Magn. Magn. Mater. **186**, 199–213 (1998).
[25] Y. Chao and J. Duan, "The Onsager-Machlup function as Lagrangian for the most probable path of a jump-diffusion process," Nonlinearity **32**, 3715–3741 (2019).
[26] T. Gao, J. Duan, and X. Li, "Fokker-Planck equations for stochastic dynamical systems with symmetric Lévy motions," Appl. Math. Comput. **278**, 1–20 (2016).
[27] X. Sun, X. Li, and Y. Zheng, "Governing equations for probability densities of Marcus stochastic differential equations with Lévy noise," Stoch. Dynam. **17**, 1750033 (2017).
[28] T. Gao, J. Duan, X. Kan, and Z. Cheng, "Dynamical inference for transitions in stochastic systems with α-stable Lévy noise," J. Phys. A Math. Theor. **49**, 294002 (2016).
[29] Z. Cheng, J. Duan, and L. Wang, "Most probable dynamics of some nonlinear systems under noisy fluctuations," Commun. Nonlinear Sci. **30**, 108–114 (2016).
[30] H. Wang, X. Chen, and J. Duan, "A stochastic pitchfork bifurcation in most probable phase portraits," Int. J. Bifurcat. Chaos **28**, 1850017 (2018).
[31] F. C. Klebaner, *Introduction to Stochastic Calculus with Applications* (World Scientific Publishing Company, 2012).
[32] J. Duan, *An Introduction to Stochastic Dynamics* (Cambridge University Press, 2015).
[33] Y. Zheng and X. Sun, "Governing equations for probability densities of stochastic differential equations with discrete time delays," Discrete Contin. Dyn. Syst. Ser. B **22**(9), 3615–3628 (2017).
[34] B. Saltzman, *Dynamical Paleoclimatology: Generalized Theory of Global Climate Change* (Elsevier, 2001).
[35] H. Kaper and H. Engler, *Mathematics and Climate* (SIAM, 2013).
[36] W. D. Nordhaus, "An optimal transition path for controlling greenhouse gases," Science **258**, 1315–1319 (1992).
[37] J. Hansen, L. Nazarenko, R. Ruedy, M. Sato, J. Willis, A. Del Genio, D. Koch, A. Lacis, K. Lo, S. Menon, T. Novakov, J. Perlwitz, G. Russell, G. A. Schmidt, and N. Tausnev, "Earth's energy imbalance: Confirmation and implications," Science **308**, 1431–1435 (2005).
[38] K. Hasselmann, "Stochastic climate models Part I. Theory," Tellus **28**, 473–485 (1976).

[39]P. D. Ditlevsen, "Anomalous jumping in a double-well potential," Phys. Rev. E **60**, 172 (1999).
[40]P. F. Hoffman, A. J. Kaufman, G. P. Halverson, and D. P. Schrag, "A neoproterozoic snowball earth," Science **281**, 1342–1346 (1998).
[41]P. Imkeller, "Energy balance models—Viewed from stochastic dynamics," in *Stochastic Climate Models* (Springer, 2001), pp. 213–240.
[42]V. Masson-Delmotte, P. Zhai, H. O. Pörtner, D. Roberts, J. Skea, P. R. Shukla, A. Pirani, W. Moufouma-Okia, C. Péan, R. Pidcock, S. Connors, J. P. R. Matthews, Y. Chen, X. Zhou *et al.*, *Global Warming of 1.5 C. An IPCC Special Report on the Impacts of Global Warming of 1.5 C above Pre-industrial Levels and Related Global Greenhouse Gas Emission Pathways, in the Context of Strengthening the Global Response to the Threat of Climate Change, Sustainable Development, and Efforts to Eradicate Poverty* (World Meteorological Organization, Geneva, 2018).
[43]Y. Huang, Y. Chao, S. Yuan, and J. Duan, "Characterization of the most probable transition paths of stochastic dynamical systems with stable Lévy noise," J. Stat. Mech. **2019**, 063204.
[44]D. Applebaum, *Lévy Processes and Stochastic Calculus* (Cambridge University Press, 2009).
[45]T. Gao, J. Duan, X. Li, and R. Song, "Mean exit time and escape probability for dynamical systems driven by Lévy noises," SIAM J. Sci. Comput. **36**, A887–A906 (2014).
[46]X. Wan and H. Yu, "A dynamic-solver–consistent minimum action method: With an application to 2D Navier-Stokes equations," J. Comput. Phys. **331**, 209–226 (2017).
[47]Y. Zheng, L. Serdukova, J. Duan, and J. Kurths, "Transitions in a genetic transcriptional regulatory system under Lévy motion," Sci. Rep. **6**, 29274 (2016).